

# Geophysical Research Letters<sup>®</sup>



## RESEARCH LETTER

10.1029/2024GL110059

### Key Points:

- We develop the first deep learning global estimates of surface ocean currents from multi-modal satellite observations
- Our deep learning method is able to map surface currents with state-of-the-art resolution and accuracy
- The diagnosed kinetic energy cascade is an order of magnitude higher compared to conventional altimetry products

### Supporting Information:

Supporting Information may be found in the online version of this article.

### Correspondence to:

S. A. Martin,  
smart1n@uw.edu

### Citation:

Martin, S. A., Manucharyan, G. E., & Klein, P. (2024). Deep learning improves global satellite observations of ocean eddy dynamics. *Geophysical Research Letters*, 51, e2024GL110059. <https://doi.org/10.1029/2024GL110059>

Received 1 MAY 2024

Accepted 16 AUG 2024

## Deep Learning Improves Global Satellite Observations of Ocean Eddy Dynamics

Scott A. Martin<sup>1</sup> , Georgy E. Manucharyan<sup>1</sup> , and Patrice Klein<sup>2,3</sup> 

<sup>1</sup>School of Oceanography, University of Washington, Seattle, WA, USA, <sup>2</sup>Jet Propulsion Laboratory, California Institute of Technology, Pasadena, CA, USA, <sup>3</sup>Laboratoire de Météorologie Dynamique, École Normale Supérieure, Paris, France

**Abstract** Ocean eddies affect large-scale circulation and induce a kinetic energy cascade through their non-linear interactions. However, since global observations of eddy dynamics come from satellite altimetry maps that smooth eddies and distort their geometry, the strength of this cascade is underestimated. Here, we use deep learning to improve observational estimates of global surface geostrophic currents and explore the implications for the cascade. By synthesizing multi-modal satellite observations of sea surface height (SSH) and temperature, we achieve up to a 30% improvement in spatial resolution over the community-standard SSH product. This reveals numerous strongly interacting eddies that were previously obscured by smoothing. In many regions, these newly resolved eddies lead to nearly an order-of-magnitude increase in the upscale kinetic energy cascade that peaks in spring and is strong enough to drive the seasonality of large mesoscale eddies. Our study suggests that deep learning can be a powerful paradigm for satellite oceanography.

**Plain Language Summary** We developed a deep learning method to estimate global maps of surface ocean currents from satellite observations with significantly improved resolution and accuracy compared to existing methods. These maps dramatically improve our ability to observe eddy dynamics and the impact of eddies on the transfer of energy between scales in the ocean. Our study suggests that deep learning can be a powerful paradigm for satellite oceanography.

### 1. Introduction

Mesoscale eddies (50–300 km) are a critical component of the global ocean circulation, transporting dynamical and biogeochemical tracers (Jayne & Marotzke, 2002; Wunsch, 1999; Zhang et al., 2014). Despite being the ocean's dominant reservoir of kinetic energy (KE), the sources and sinks of mesoscale eddy KE remain poorly constrained (Ferrari & Wunsch, 2009). One major process affecting mesoscale KE is the transfer of KE between scales by non-linear eddy interactions, known as the KE cascade (Aluie et al., 2018; Klein et al., 2019; Scott & Wang, 2005). There is growing evidence that non-linear eddy interactions induce a strongly seasonal upscale KE cascade, KE transfer from small to large scales, that is intensified in winter and spring (Ajayi et al., 2021; Balwada et al., 2022; Lawrence & Callies, 2022; Naveira Garabato et al., 2022; Qiu et al., 2014; Sasaki et al., 2014; Schubert et al., 2020, 2023; Steinberg et al., 2022; Storer et al., 2023; Uchida et al., 2017). The strength of non-linear eddy interactions and the KE cascade are set by the vorticity and strain (Aluie et al., 2018; Klein et al., 2019), which are sensitive to the geometry of eddies. There is thus a need for global observations of eddies with sufficient resolution to accurately diagnose vorticity and strain - this motivates our study.

Satellite observations of eddy surface expressions are a powerful observing system for eddy dynamics since satellites resolve a wide range of scales compared to in situ observations (Klein et al., 2019), however, inferring surface currents from satellite observables is challenging. Satellite altimetry allows the estimation of eddies by mapping their expression in sea surface height (SSH), which is used to estimate surface geostrophic currents (Chelton et al., 2001). Conventional altimeters measure SSH and resolve mesoscale eddies along each satellite's track (Dufau et al., 2016) but leave large gaps between tracks that must be interpolated to diagnose eddy dynamics. Meanwhile, satellites observe high-resolution 2D snapshots of sea surface temperature (SST) but there are gaps due to clouds and the relationship between SST and surface currents is complex (Isern-Fontanet et al., 2006, 2014; Rio et al., 2016).

Conventionally, surface currents are estimated either via data assimilation (DA) (Le Guillou et al., 2021, 2023; Lellouche et al., 2021) or objective analysis (OA) of SSH (Taburet et al., 2019; Ubelmann et al., 2015, 2021, 2022). DA provides 3D state estimates approximately consistent with the physics of a numerical model, typically

© 2024, The Author(s).

This is an open access article under the terms of the [Creative Commons Attribution-NonCommercial-NoDerivs License](#), which permits use and distribution in any medium, provided the original work is properly cited, the use is non-commercial and no modifications or adaptations are made.

a general circulation model (GCM). However, state-of-the-art DA systems (Lellouche et al., 2021) use GCM resolutions that only partially resolve mesoscale dynamics and so suffer high errors in SSH and surface currents at mesoscales due to unresolved eddy dynamics and the lack of high-resolution 3D in-situ observations. In contrast, OA allows to estimate only the 2D SSH field using a statistical approach (Taburet et al., 2019; Ubelmann et al., 2015, 2021, 2022), from which currents can be estimated through geostrophy and further corrections for winds (Rio et al., 2014), equatorial dynamics (Lagerloef et al., 1999), cyclo-geostrophy (Cao et al., 2023; Penven et al., 2014), or potentially using machine learning (Sinha & Abernathey, 2021; Xiao et al., 2023). Surface currents derived from OA SSH fields give eddy amplitudes and configurations more consistent with observations than DA since they are not biased by unresolved dynamics. However, OA is a fundamentally statistical approach that does not guarantee a physically consistent reconstruction and biases in the covariance models used in OA could bias the reconstructions. OA artificially suppresses variance at smaller scales, smoothing and distorting eddies (Ballarotta et al., 2019). This leads to a significant underestimation of crucial dynamical quantities, like vorticity and strain.

Deep learning has emerged as an alternative approach for estimating surface currents. Many proof-of-concept studies demonstrate that neural networks can be trained to map SSH or surface currents from altimeter observations, through either ‘simulation learning’ using synthetic data from high-resolution GCMs (Archambault et al., 2024; Beauchamp et al., 2022; Buongiorno Nardelli et al., 2022; Fablet et al., 2021, 2023; Febvre et al., 2024; Kugusheva et al., 2024; Manucharyan et al., 2021; Thiria et al., 2023) or ‘observation-only learning’ from real-world satellites (Archambault et al., 2023; Martin et al., 2023). Deep learning allows the optimal mapping to emerge objectively from the data, unlike OA which prescribes linear covariance models (Taburet et al., 2019), and allows to use SST observations as an additional input to improve the mapping between altimeter observations (Archambault et al., 2023, 2024; Buongiorno Nardelli et al., 2022; Fablet et al., 2023; Martin et al., 2023). Simulation learning showed promising results on synthetic observations in proof-of-concept studies. However, transferring these methods to real-world observations remains a challenge since GCMs are not exact analogs of the real world and neural networks behave unpredictably when applied to data different from that used during training. This domain gap can be partly addressed through fine-tuning on real-world observations (Archambault et al., 2024; Febvre et al., 2024). Fundamentally, simulation learning blurs the boundary between observations and GCMs, much like DA. In contrast to simulation learning, observation-only learning, analogous to OA, is directly applicable to real-world observations and is uncontaminated with GCM biases. This comes at the expense of smoothing some smaller-scale features due to the limited resolution of real-world observations. Nonetheless, regional proof-of-concept studies have shown observation-only learning can give SSH maps with higher resolution than OA, leading to significant improvements in the estimation of vorticity and strain (Archambault et al., 2023; Martin et al., 2023).

Extending regional proof-of-concept studies to global SSH mapping poses a significant challenge for deep learning because the global ocean exhibits spatiotemporally diverse dynamics. Given the sparsity of the altimetry record for observation-only learning, it remains to be demonstrated that a neural network can generalize across all dynamical regimes. We hypothesize that observation-only learning can be used to create global SSH maps with enhanced resolution, and that this will radically improve global observations of vorticity and strain - and hence of non-linear eddy dynamics. Here, we develop the first global deep learning estimates of SSH and surface currents. We evaluate the accuracy of the SSH maps, their ability to resolve vorticity and strain, and explore the resulting KE cascade. By disseminating our new global SSH product, we hope to enable more accurate studies of eddy dynamics and their impact on general ocean circulation, marine ecosystems, and climate.

## 2. Methods

### 2.1. NeurOST: Global SSH Maps From Altimetry and SST Using Deep Learning

We train a neural network to map SSH from sparse altimeter observations (E.U. Copernicus Marine Service Information (CMEMS), 2024b; E.U. Copernicus Marine Service Information (CMEMS), 2024a) and gridded SST (JPL MUR MEaSUREs Project, 2015). Our approach (Figure 1), builds upon that described in our recent proof-of-concept study (Martin et al., 2023) and is described in full in S.I. S1.1-5 in Supporting Information S1.

We use ‘self-supervised’ learning, taking a time series of altimeter observations within a local subdomain (30 days by 960 km by 960 km) from all but one of the available altimeters alongside the corresponding SST as input to a neural network tasked with reconstructing 2D SSH. The objective minimized during training is the

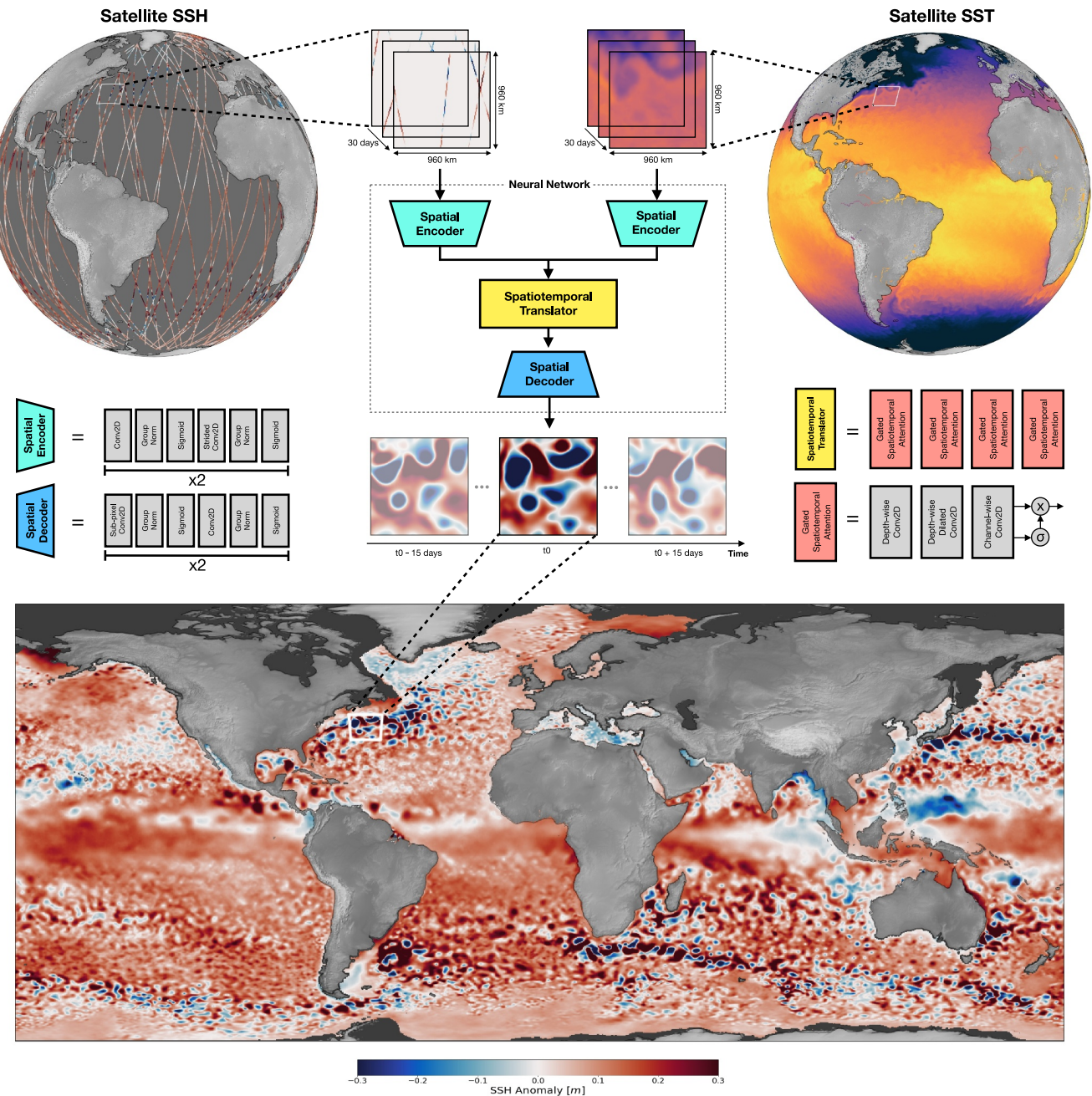


**Figure 1.** Schematic of NeurOST SSH-SST method for mapping SSH from satellite altimetry and SST.

mean square error of the mapped SSH calculated against the withheld altimeter. We restrict the mapping to local subdomains since eddy dynamics are local, so a global ‘field of view’ is likely unnecessary to reconstruct eddies in any local subdomain.

We use kernel-weighted averaging to combine thousands of overlapping subdomain SSH maps together into a single global SSH map (S.I. S1.5 and Callaham et al. (2019)). Using a large set of subdomain examples drawn from across the globe, we train a single network to map SSH in all regions, achieving generalization across diverse regional dynamics. By training a single global network rather than an ensemble of bespoke regional networks we avoid arbitrarily dividing the globe into regions and learn a general and robust SSH mapping. The network was trained on observations from 2010 to 2023, with 2019 withheld for validation (Figure S8 in Supporting Information S1).

We refer to our method as ‘NeurOST (SSH-SST)’ (Neural Ocean Surface Topography). To assess the value of SST we also trained a network to map SSH from altimetry alone; ‘NeurOST (SSH)’.

## 2.2. Estimating Surface Currents From SSH

Large-scale currents satisfy geostrophic balance, allowing surface currents to be estimated from SSH through geostrophy (S.I. Equation 1 in Supporting Information S1). The limitations of geostrophy and potential empirical ageostrophic corrections (Cao et al., 2023; Lagerloef et al., 1999; Penven et al., 2014; Rio et al., 2014) are discussed in S.I. S1.1 Supporting Information S1 where we also show diagnostics of eddy dynamics (e.g., KE cascade) are only weakly sensitive to the cyclo-geostrophy correction (Penven et al., 2014). Thus, throughout this manuscript, surface currents were calculated using geostrophy.

## 2.3. SSH Mapping Evaluation: Observing System Experiment (OSE)

We employ an observing system experiment (OSE) to evaluate SSH maps. Comparisons to existing methods are achieved using an Ocean Data Challenge (Metref & Ballarotta, 2023; Metref et al., 2023) in which developers of different methods implement them on a common experiment. In the OSE used here, we create global SSH maps for 2019 using all altimeters apart from Saral/AltiKa that is used for evaluation. Accuracy is evaluated using root mean square error (RMSE), and we quantify the maps’ effective spatial resolution (the smallest resolved wavelength) following Ballarotta et al. (2019). We compare NeurOST to the community-standard ‘DUACS’ product (Le Traon et al., 1998; Taburet et al., 2019) as well as to the ‘MIOST’ method (Ballarotta et al., 2023; Ubelmann et al., 2021). Surface geostrophic currents are evaluated using drifters (Copernicus Marine in situ TAC, 2024). Additionally, we compare NeurOST to proof-of-concept methods in the Gulf Stream Extension using a similar Ocean Data Challenge that was regional in scope (Ballarotta et al., 2021) (S.I. S1.6-7 Supporting Information S1).

## 2.4. Eddy Dynamics Evaluation: Observing System Simulation Experiment (OSSE)

While the OSE evaluates SSH maps, we cannot use it to evaluate eddy dynamics (vorticity and strain) inferred from SSH as this requires the full 2D eddy field. We therefore conduct an observing system simulation experiment (OSSE) where we generate synthetic altimeter observations from the 1/12° GLORYS reanalysis (Lellouche et al., 2021; E.U. Copernicus Marine Service Information (CMEMS), 2024c) and use them in combination with GLORYS SST as input to NeurOST, with no re-training on GLORYS. We compare the resulting NeurOST maps to the 2D ground-truth from GLORYS to evaluate eddy dynamics diagnostics, specifically surface geostrophic currents and vorticity for which we define skill scores representing the fraction of variance explained (S.I. S1.11 Supporting Information S1). This point-wise comparison to GLORYS cannot be made for DUACS since this method is not open source, preventing its implementation on simulated observations.

## 2.5. Kinetic Energy Cascade Diagnosis

We use NeurOST surface geostrophic currents to diagnose the KE cascade in a range of regions through coarse-graining (Aluie et al., 2018; Storer & Aluie, 2023; Storer et al., 2022, 2023). The KE cascade is diagnosed through the spectral KE flux, which quantifies KE transfer from larger to smaller scales at each wavelength. A positive flux indicates a downscale (forward) cascade, whereas a negative value indicates an upscale (inverse) cascade (S.I. S1.12 Supporting Information S1).

# 3. Results

## 3.1. State-Of-The-Art Global SSH Maps Using Deep Learning

Our global SSH maps (NeurOST SSH-SST) show rich dynamical structures associated with western boundary currents, abundant mesoscale eddies in the extratropics, and large-scale equatorial waves in the tropics (Figure 1).

The effective resolution of our maps is improved compared to DUACS throughout the global ocean, with a pronounced improvement in western boundary currents and the subtropics where we resolve wavelengths 30% smaller (Figures 2b and 2d and Table S1 in Supporting Information S1). The global RMSE of the mapped SSH is 6% lower than DUACS, while reductions in the RMSE of small mesoscales (70–250 km wavelengths) reach 20% in eddy-rich regions (Figures 2a– 2c and 2e and Table S1 in Supporting Information S1). Similarly, NeurOST

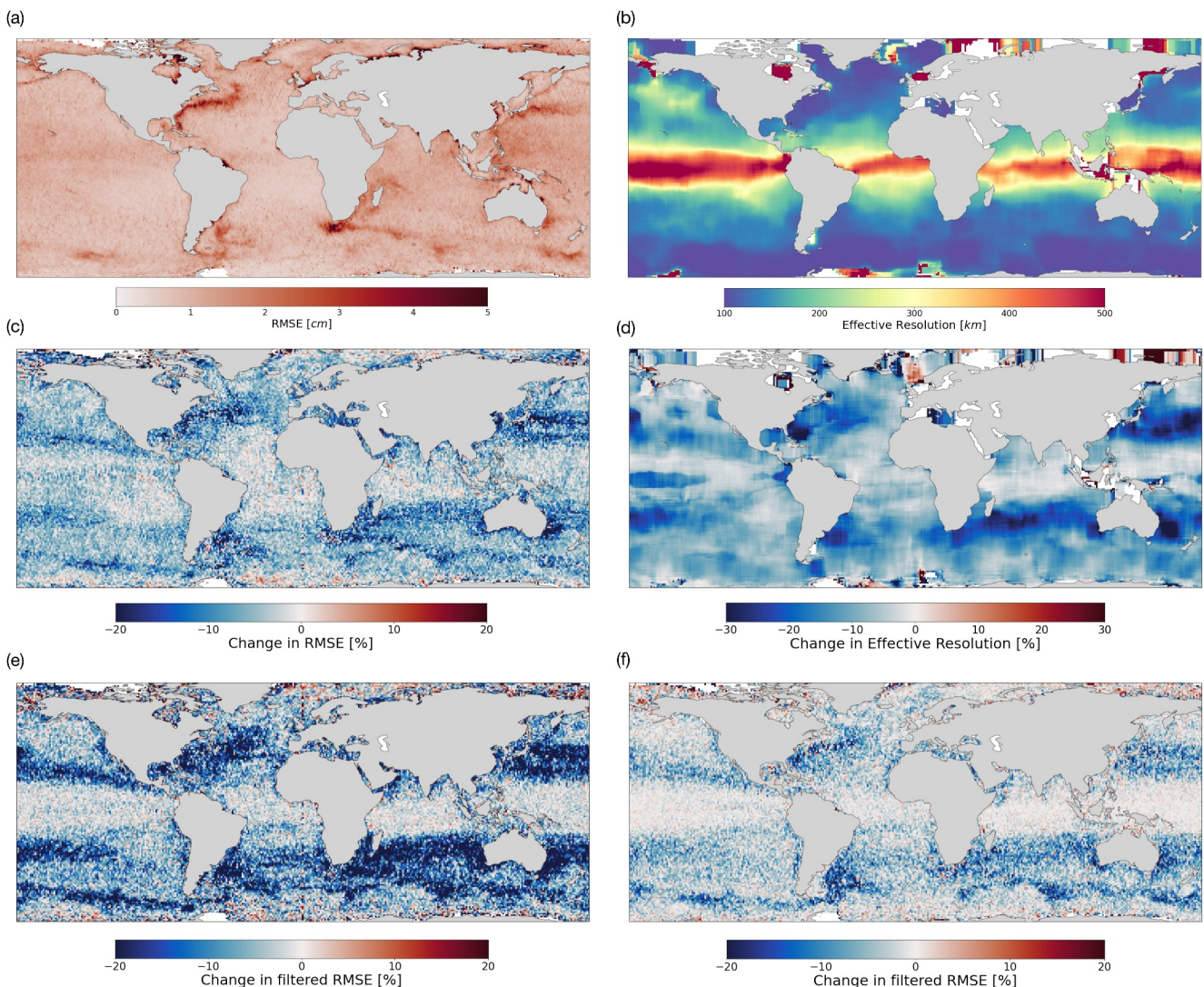


**Figure 2.** (a) RMSE of NeurOST SSH-SST compared to withheld altimeter. (b) Smallest resolved wavelengths (effective resolution) of NeurOST SSH-SST. (c) Change in RMSE of NeurOST SSH-SST compared to DUACS. (d) Change in effective resolution of NeurOST SSH-SST compared to DUACS. (e) Change in RMSE of small-scale (70–250 km) signals of NeurOST SSH-SST compared to DUACS. (f) Change in RMSE of small-scale signals of NeurOST SSH-SST compared to NeurOST SSH. Blue colors indicate a relative decrease in panels (c)–(f).

outperforms MIOST in almost all regions, especially for small mesoscales, making NeurOST state-of-the-art in global SSH mapping (Figure S1 and Table S1 in Supporting Information S1).

Using SST improves the mapping of SSH throughout the global ocean (Figure 2f and Table S1 in Supporting Information S1). To assess the utility of SST, we compare the performance of NeurOST with and without SST. The mapping of small mesoscales is improved using SST, especially in the extratropics where mesoscale SSH and SST are correlated (Cornillon et al., 2019) (Figure 2f and Table S1 in Supporting Information S1). SST is especially impactful when few altimeters are available (Table S3 in Supporting Information S1). While observations from six altimeters were used to create the maps compared above, for much of the altimetry era only two altimeters were operational, causing eddies in DUACS to be severely smoothed. We evaluated our network using only two altimeters and found that in most regions NeurOST SSH-SST with just two altimeters yields higher-resolution SSH than DUACS achieves with six (Table S3 in Supporting Information S1). This highlights the potential of deep learning and SST to extract maximum value from the 30-year altimetry record.

NeurOST maps SSH across all regions, unlike prior studies that trained bespoke region-specific networks. While regional networks (Febvre et al., 2024; Martin et al., 2023) in the Gulf Stream offer marginally improved SSH

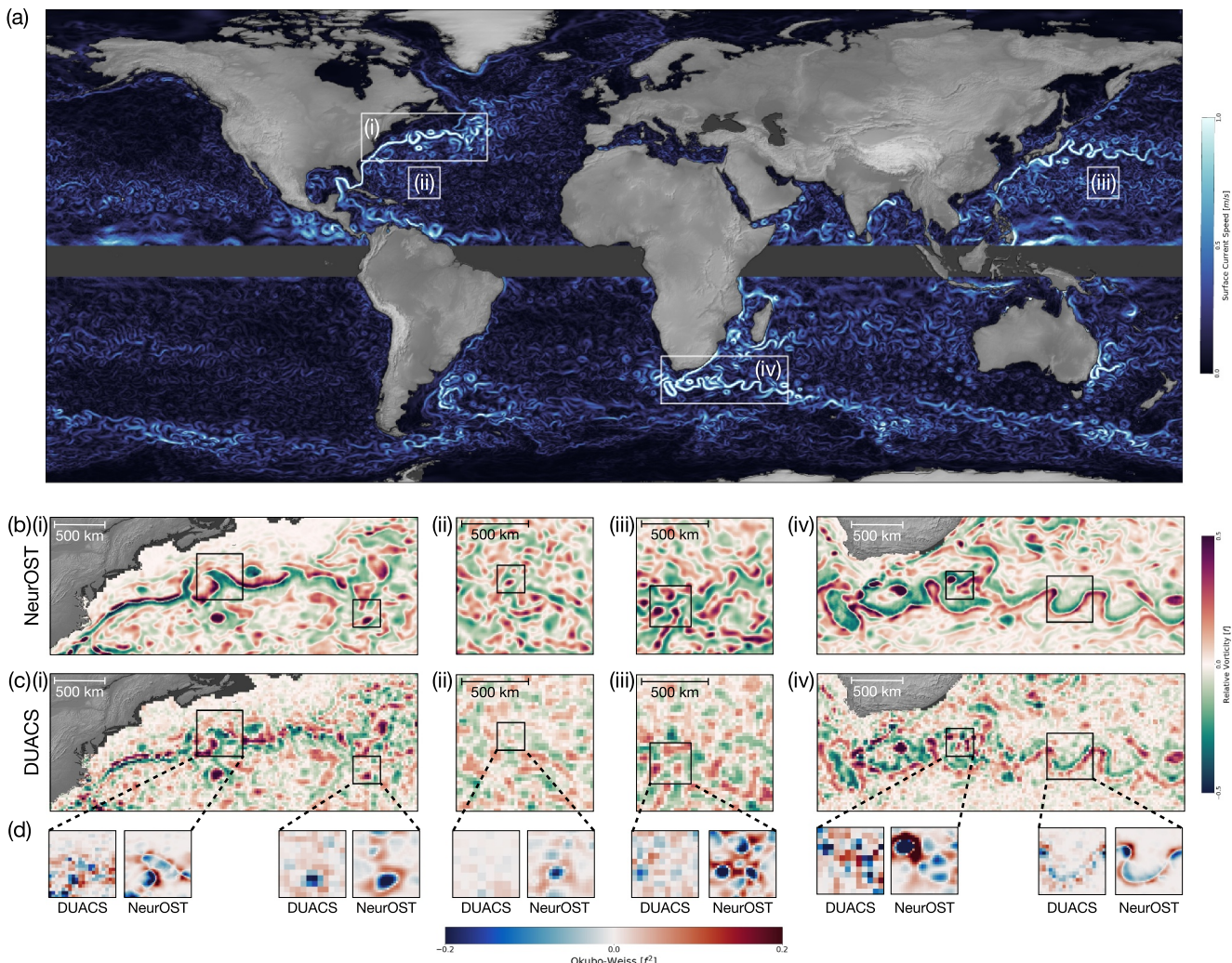


**Figure 3.** (a) Surface geostrophic current speed on 1 March 2019 derived from SSH maps made using NeurOST SSH-SST. (b) Relative vorticity from NeurOST SSH-SST. (c) Relative vorticity from DUACS. (d) Zoomed insets of Okubo-Weiss quantity for DUACS and NeurOST SSH-SST.

mapping compared to NeurOST (Ballarotta et al., 2021) (Table S2 in Supporting Information S1), fine-tuning on a smaller set of observations from the Gulf Stream (S.I. S1.6 Supporting Information S1) brings NeurOST in line with state-of-the-art regional networks (Table S2 in Supporting Information S1). This shows the potential for further refinement of NeurOST by users interested only in a single region.

Surface geostrophic currents from our maps are more accurate when evaluated with drifter observations. NeurOST reduces the RMSE of surface currents significantly across the global ocean, especially in the subtropics, where RMSE is reduced by 20% compared to DUACS (Figure S2 in Supporting Information S1). Discrepancies between the mapped currents and drifter observations are due to both the accuracy of the mapped geostrophic current and the degree to which real-world currents are in geostrophic balance. Nonetheless, this large reduction in RMSE demonstrates the significant improvement in the mapped currents.

### 3.2. Improved Physical Realism of Mesoscale Eddies

Calculating vorticity and strain from the surface current maps appears to show a significant qualitative improvement in the realism of eddy dynamics in NeurOST (Figures 3b–3d and Movie S1). NeurOST vorticity shows abundant small mesoscale eddies with clear boundaries, many of which are absent in DUACS (Figures 3b and 3c). A contrasting view of eddy dynamics emerges when comparing the eddy evolution: eddies appear to uniformly propagate westward in DUACS, while NeurOST eddies exhibit strong non-linear interactions that

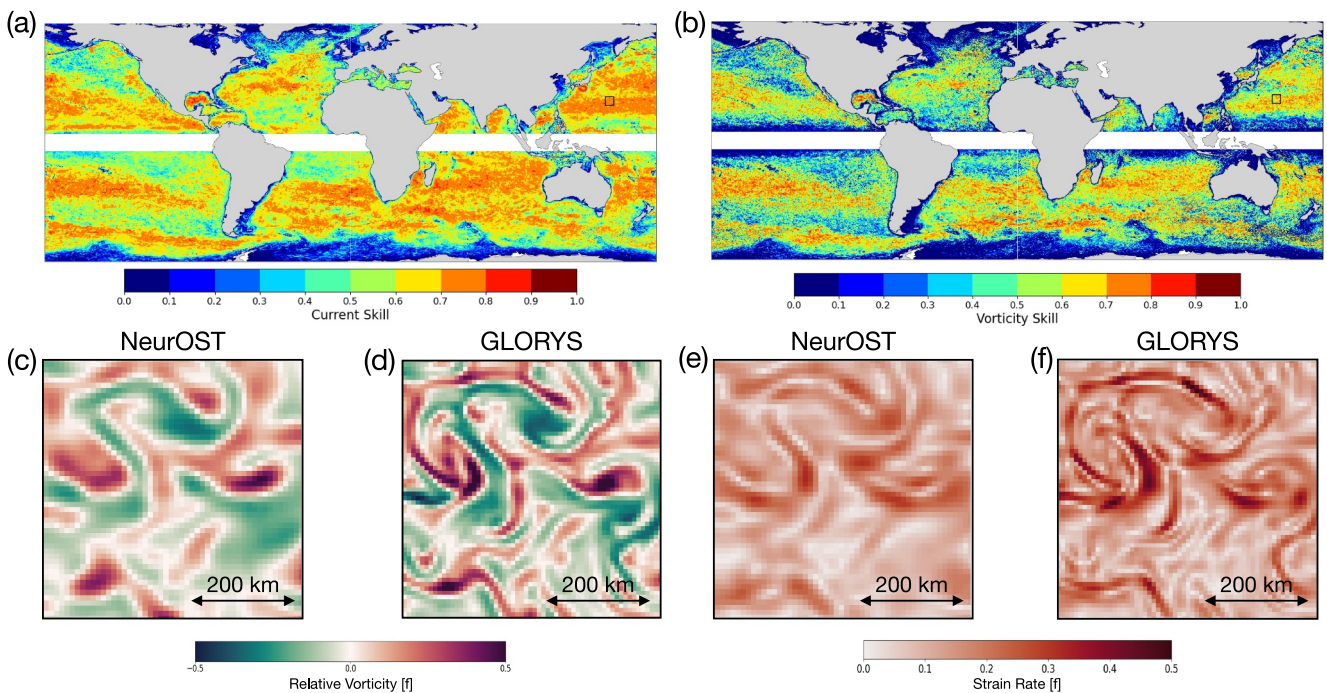


**Figure 4.** NeurOST SSH-SST reconstruction skill (explained variance) in GLORYS OSSE for (a) surface geostrophic currents and (b) vorticity. Snapshots of (c), (d) vorticity and (e), (f) strain from Subtropical North Pacific (boxed region in a and b) for NeurOST and GLORYS on 26 Feb 2019.

deform each other's vorticity cores, causing filamentation (Supplementary Movie S1). These better-resolved non-linear eddy interactions also manifest in the higher strain rate between eddies seen in NeurOST, evidenced by regions of highly positive Okubo-Weiss quantity (Figure 3d, S.I. S1.10 in Supporting Information S1). Increased strain has important implications for eddy dynamics since it is associated with enhanced frontogenesis (Hoskins, 1982; Siegelman et al., 2020) and a stronger KE cascade (Aluie et al., 2018). While vorticity and strain appear qualitatively more realistic in NeurOST, their accuracy cannot be quantified using along-track SSH observations. To demonstrate that NeurOST does not introduce artificial eddies, we test its ability to reconstruct vorticity using synthetic observations from a GCM (Section 2.4).

NeurOST, trained on real-world observations and applied now to synthetic observations from GLORYS, skillfully reconstructs surface currents, especially in the subtropics and western boundary currents, explaining over 70% of the variance (Figure 4a). Its skill deteriorates somewhat in regions of low variability, at high latitudes, and near coasts, where the observational training data is likely to significantly differ from the GLORYS simulation. Since vorticity is sensitive to small-scale SSH features, its overall reconstruction skill is slightly lower than that for surface currents. Nonetheless, NeurOST reconstructs a remarkable 50%–80% of vorticity variance throughout the subtropics and western boundary currents. Comparing spatial patterns of vorticity and strain, it is clear that NeurOST misses smaller-scale filaments but skillfully reconstructs larger eddies and some larger filaments and is not prone to creating artificial eddies (Figures 4c–4f and Supplementary Movie S2). NeurOST can reconstruct features as small as 50 km (see filaments in Figures 4c–4f). Thus, NeurOST can reasonably well reconstruct the 2D vorticity and strain fields despite being trained only on real-world along-track SSH observations and never on real or simulated vorticity/strain.

Since GLORYS contains finer-scale vorticity features than NeurOST, it can be used to estimate the KE cascade (see Storer et al. (2023) and Figure S7 in Supporting Information S1). However, there is a qualitative difference in eddy dynamics between GLORYS and NeurOST that clearly manifests in small-scale vorticity features. In GLORYS, vorticity features are dominated by persistent filaments, whereas in NeurOST there is an abundance of smaller-scale coherent eddies with less prominent filaments (Supplementary Movie S1). This difference could be due to the relatively coarse grid of GLORYS ( $1/12^\circ$ ) that does not resolve the generation of small-scale eddies by submesoscale instabilities in the mixed layer, which are known to be prominent in winter. In such coarse-resolution models, large eddies stir vorticity to form small-scale filaments, but they can artificially persist and

grow, being constrained only by numerical or specified model diffusion. In reality, the presence of small-scale eddies can disrupt this filamentation by large-scale eddies, and filaments often become unstable and form submesoscale eddies (e.g., Taylor and Thompson (2023)). Since there are no ground-truth observations of vorticity, one cannot definitively establish whether there is excessive filamentation in GLORYS or whether NeurOST introduces artificial eddies at small scales. However, looking at the NeurOST reconstruction of GLORYS (Section 2.4), NeurOST appears to provide a coarse-grained view of GLORYS, showing no evidence of artificial small-scale eddies being introduced (compare Supplementary Movies S1 & S2). Furthermore, when reconstructing real-world SSH and surface currents, NeurOST also has significantly lower errors than GLORYS (Figure S3 and Table S1 in Supporting Information S1). With increased confidence that NeurOST provides a better estimation of real-world ocean eddy dynamics, we now proceed to explore its impact on our understanding of the KE cascade and seasonality of mesoscale eddies.

### 3.3. Seasonal Kinetic Energy Cascade

A distinct seasonality in eddy dynamics emerges in NeurOST that was largely absent in DUACS, with smaller scale eddies peaking in intensity in winter and spring. The mesoscale KE and strain rate throughout the subtropics are 50%–100% higher in NeurOST than in DUACS in winter/spring, whereas they are comparable in summer/autumn (Figure S4 and S5 in Supporting Information S1). We explore this newly resolved seasonality by focusing on the Subtropical North Pacific, which was the subject of prior studies of eddy seasonality (Qiu et al., 2014).

Eddy dynamics from NeurOST are strongly seasonal in the Subtropical North Pacific, with enstrophy (the variance of vorticity) peaking in winter/spring implying intensified small-scale eddies (Figure 5a). This strong wintertime peak in enstrophy in NeurOST is qualitatively consistent with submesoscale-resolving simulations (Qiu et al., 2014). The seasonality of small-scale eddies is corroborated by the KE wavenumber spectrum (S.I. S1.13 Supporting Information S1) that has a shallower slope ( $\approx k^{-2}$ ) in winter/spring than in summer/autumn ( $\approx k^{-3}$ ) (Figure 5b), meaning energy is more concentrated at small scales in winter/spring. Notably, the peak in KE for small-scales (<125 km) leads that for larger scales by 2 months (Figure 5c). It has been hypothesized that the delayed large-scale KE peak may partly be driven by an upscale KE cascade from submesoscales, which are most energetic during winter (Qiu et al., 2014; Sasaki et al., 2014). However, this hypothesis has not been confirmed using observations since low-resolution products like DUACS fail to resolve the small-scale eddies that proliferate in winter/spring (Figures 5a and 5c), and hence underestimate the KE cascade (Arbic et al., 2013).

The KE cascade from NeurOST is upscale throughout the mesoscale range in the Subtropical North Pacific, has a strong springtime peak, and is dramatically stronger than in DUACS (Figure 5d). Although some KE sources and sinks cannot be derived from surface currents (S.I. S1.12 in Supporting Information S1), the magnitude of the cascade appears more than sufficient to drive the increase in large-scale KE observed over winter/spring (Figure 5e). In contrast, the overly smooth DUACS product significantly underestimates the springtime KE cascade, obscuring the seasonality of the cascade and its role in driving the large-scale peak (Figure 5e). The cascade also appears to play a crucial role in driving large-scale seasonality in other subtropical regions (Figure S6 in Supporting Information S1). At scales resolved in our study, there are no ground-truth data for the KE cascade to compare against (Balwada et al., 2022; Naveira Garabato et al., 2022; Yoo et al., 2018), but recent studies of along-track altimetry provide indirect evidence for the seasonal upscale KE cascade observed here (Lawrence & Callies, 2022; Schubert et al., 2023; Steinberg et al., 2022). Note that in western boundary currents, lateral KE advection appears to dominate the cascade (Figure S6 in Supporting Information S1), and there is likely a substantial KE injection by instabilities of large-scale currents that cannot be diagnosed from SSH. Note that NeurOST (SSH-SST) shows a stronger seasonality in the cascade than NeurOST (SSH), likely since small wintertime eddies are hard to capture without tracking their expression in SST (Figure S12 in Supporting Information S1).

## 4. Conclusions

Our high-resolution SSH maps generated using deep learning represent a large stride forward for the global observation of ocean eddy dynamics, providing state-of-the-art global surface currents. Trained on real-world observations alone, NeurOST allows to diagnose eddy dynamics with greater physical realism than from existing altimetry products. NeurOST revealed the crucial role of non-linear eddy dynamics and their associated KE cascade in driving the seasonality of mesoscale eddies in many parts of the global ocean, highlighting the

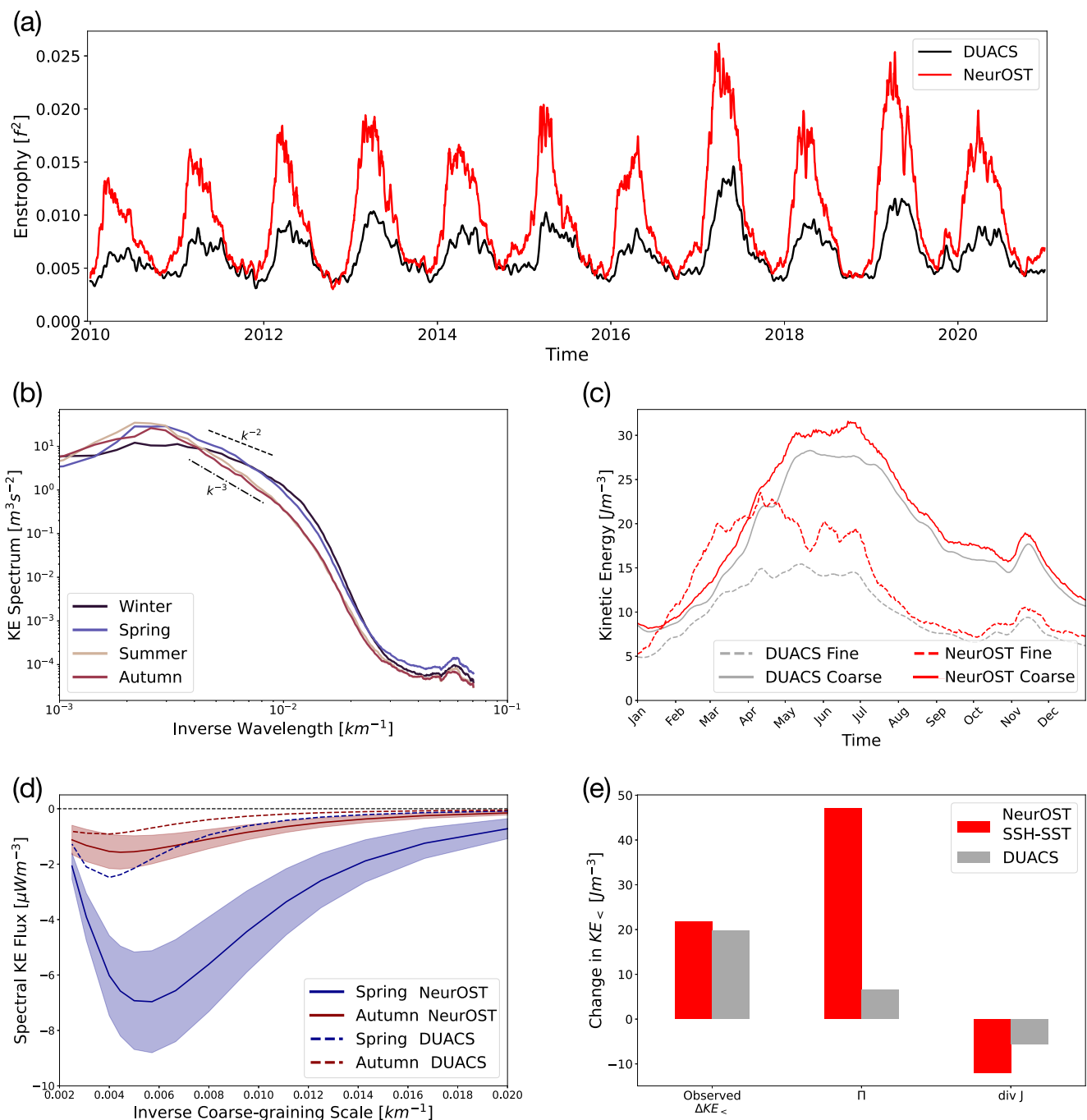


**Figure 5.** (a) Enstrophy time-series in the Subtropical North Pacific for NeurOST SSH-SST and DUACS. (b) KE spectra from NeurOST SSH-SST split by season. (c) Time-series of coarse- and fine-scale KE (above and below 125 km coarse-graining scale respectively) from NeurOST SSH-SST (red) and DUACS (gray). (d) KE cascade from NeurOST SSH-SST maps for the seasons of maximum (Spring) and minimum (Autumn) upscale cascade (solid line: mean, shading: standard deviation). Dashed lines are the mean cascades from DUACS. (e) Change in coarse-scale KE ( $KE_{<}$ ) from the winter-time minimum to the summer-time maximum compared to the diagnosed contributions of the KE cascade ( $-\int \Pi dt$ ), and the spatial transport of coarse-scale KE ( $-\nabla \cdot J dt$ ) from NeurOST SSH-SST (red) and DUACS (gray) (S.I. S1.12 in Supporting Information S1).

importance of resolving small-scale eddy dynamics in ocean models. Alongside this manuscript, we publish a NeurOST SSH product (OSTST, 2024) to facilitate future studies of eddy dynamics and the impacts of eddies on climate and marine ecosystems.

Despite the improved resolution of NeurOST, it does not yet resolve submesoscale eddies, smoothing scales below  $O(100\text{ km})$  (Table S4 in Supporting Information S1). Hence, the strength of the upscale cascade is likely still underestimated (Figure S7 in Supporting Information S1), and the potential presence of a downscale cascade at submesoscales cannot be quantified. The recently launched Surface Water and Ocean Topography (SWOT) satellite, the first wide-swath altimeter (Fu et al., 2024; Morrow et al., 2019), provides unprecedented 2D submesoscale-resolving SSH snapshots that could help characterize the KE cascade at submesoscales (Carli et al., 2023; Klein et al., 2019). However, SWOT observations present new challenges for inferring currents from SSH due to the presence of unbalanced submesoscale SSH variability and the mismatch between fast-evolving submesoscale dynamics and SWOT's long return times (Gaultier et al., 2016; Torres et al., 2018). Deep learning methods to address these issues are under development and show promise (Febvre et al., 2022; Gao et al., 2024; Wang et al., 2022). As satellite oceanography enters a new submesoscale-resolving era (Fu et al., 2024; Morrow et al., 2019), further development of deep learning methods will be crucial to best monitor surface currents and other essential climate variables, like SST (Agabin et al., 2024; Goh et al., 2023).

## Data Availability Statement

The NeurOST maps for 2019 with 1 satellite altimeter withheld for validation are available (Martin, 2024b). A longer time-series of NeurOST maps using all available altimeters intended for users is available through NASA PO. DAAC (OSTST, 2024). We used MUR SST data from PO. DAAC (JPL MUR MEASURE Project, 2015) and the altimeter, surface drifter observations, and GLORYS reanalysis data from CMEMS (E.U. Copernicus Marine Service Information (CMEMS), 2024b; E.U. Copernicus Marine Service Information (CMEMS), 2024a; Copernicus Marine in situ TAC, 2024; E.U. Copernicus Marine Service Information (CMEMS), 2024c). Ocean Data Challenges for global SSH mapping ([https://github.com/ocean-data-challenges/2023a\\_SSH\\_mapping\\_OSE](https://github.com/ocean-data-challenges/2023a_SSH_mapping_OSE)) and for the Gulf Stream Extension ([https://github.com/ocean-data-challenges/2021a\\_SSH\\_mapping\\_OSE](https://github.com/ocean-data-challenges/2021a_SSH_mapping_OSE)) are on GitHub. In Table S3 in Supporting Information S1 we also use data from Febvre (2023) and Archambault (2023). NeurOST code is available (Martin, 2024a) and for coarse-graining we used FlowSieve (Storer & Aluie, 2023).

## Acknowledgments

The research was funded by NASA Grant 80NSSC21K1187. P.K. acknowledges support from the SWOT Science Team and the QuikSCAT mission. We thank the creators of the Ocean Data Challenges, especially Sammy Metref and Maxime Ballarotta. We acknowledge helpful discussions with Steven Brunton, Jinbo Wang, Brian Arbic, Quentin Febvre, Tom Farrar, J. Xavier Prochaska, Peter Cornillon, and Christian Buckingham. Computational resources supporting this work were provided by the NASA High-End Computing (HEC) Program through the NASA Advanced Supercomputing (NAS) Division at Ames Research Center. We thank Julian Mak and two anonymous reviewers for helping to improve the manuscript.

## References

- Agabin, A., Prochaska, J. X., Cornillon, P. C., & Buckingham, C. E. (2024). Mitigating masked pixels in a climate-critical ocean dataset. *Remote Sensing*, 16(13), 2439. <https://doi.org/10.3390/rs16132439>
- Ajayi, A., Le Sommer, J., Chassignet, E. P., Molines, J.-M., Xu, X., Albert, A., & Dewar, W. (2021). Diagnosing cross-scale kinetic energy exchanges from two submesoscale permitting ocean models. *Journal of Advances in Modeling Earth Systems*, 13(6), e2019MS001923. <https://doi.org/10.1029/2019ms001923>
- Aluie, H., Hecht, M., & Vallis, G. K. (2018). Mapping the energy cascade in the North Atlantic Ocean: The coarse-graining approach. *Journal of Physical Oceanography*, 48(2), 225–244. <https://doi.org/10.1175/jpo-d-17-0100.1>
- Arbic, B. K., Polzin, K. L., Scott, R. B., Richman, J. G., & Shriner, J. F. (2013). On eddy viscosity, energy cascades, and the horizontal resolution of gridded satellite altimeter products. *Journal of Physical Oceanography*, 43(2), 283–300. <https://doi.org/10.1175/jpo-d-11-0240.1>
- Arbic, B. K., Scott, R. B., Chelton, D. B., Richman, J. G., & Shriner, J. F. (2012). Effects of stencil width on surface ocean geostrophic velocity and vorticity estimation from gridded satellite altimeter data. *Journal of Geophysical Research*, 117(C3). <https://doi.org/10.1029/2011jc007367>
- Archambault, T. (2023). Code repository for the article: Multimodal unsupervised spatio-temporal interpolation of satellite ocean altimetry maps. [Dataset]. *GitLab*. Retrieved from <https://gitlab.lip6.fr/archambault/visapp2023>
- Archambault, T., Filoche, A., Charantonis, A., & Béreziat, D. (2024). Pre-training and fine-tuning attention based encoder decoder improves sea surface height multi-variate inpainting. In *VISAPP*.
- Archambault, T., Filoche, A., Charantonis, A., & Béreziat, D. (2023). Multimodal unsupervised spatio-temporal interpolation of satellite ocean altimetry maps. In *VISAPP*.
- Ballarotta, M., Metref, S., Albery, A., Cosme, E., Beauchamp, M., & Le Guillou, F. (2021). Ocean data challenges: 2021a SSH mapping OSE. [https://github.com/ocean-data-challenges/2021a\\_SSH\\_mapping\\_OSE](https://github.com/ocean-data-challenges/2021a_SSH_mapping_OSE)
- Ballarotta, M., Ubelmann, C., Pujol, M.-I., Taburet, G., Fournier, F., Legeais, J.-F., et al. (2019). On the resolutions of ocean altimetry maps. *Ocean Science*, 15(4), 1091–1109. <https://doi.org/10.5194/os-15-1091-2019>
- Ballarotta, M., Ubelmann, C., Veillard, P., Prandi, P., Etienne, H., Mulet, S., et al. (2023). Improved global sea surface height and current maps from remote sensing and in situ observations. *Earth System Science Data*, 15(1), 295–315. <https://doi.org/10.5194/essd-15-295-2023>
- Balwada, D., Xie, J.-H., Marino, R., & Feraco, F. (2022). Direct observational evidence of an oceanic dual kinetic energy cascade and its seasonality. *Science Advances*, 8(41), eabq2566. <https://doi.org/10.1126/sciadv.abq2566>
- Beauchamp, M., Febvre, Q., Georgenthum, H., & Fablet, R. (2022). 4DVarNet-SSH: End-to-end learning of variational interpolation schemes for nadir and wide-swath satellite altimetry. *Geoscientific Model Development Discussions*, 2022, 1–37.
- Buongiorno Nardelli, B., Cavaliere, D., Charles, E., & Ciani, D. (2022). Super-resolving ocean dynamics from space with computer vision algorithms. *Remote Sensing*, 14(5), 1159. <https://doi.org/10.3390/rs14051159>
- Callahan, J. L., Maeda, K., & Brunton, S. L. (2019). Robust flow reconstruction from limited measurements via sparse representation. *Physical Review Fluids*, 4(10), 103907. <https://doi.org/10.1103/physrevfluids.4.103907>
- Cao, Y., Dong, C., Stegner, A., Bethel, B. J., Li, C., Dong, J., et al. (2023). Global sea surface cyclogeostrophic currents derived from satellite altimetry data. *Journal of Geophysical Research: Oceans*, 128(1), e2022JC019357. <https://doi.org/10.1029/2022jc019357>

- Carli, E., Morrow, R., Vergara, O., Chevrier, R., & Renault, L. (2023). Ocean 2D eddy energy fluxes from small mesoscale processes with SWOT. *Ocean Science*, 19(5), 1413–1435. <https://doi.org/10.5194/os-19-1413-2023>
- Chelton, D. B., Ries, J. C., Haines, B. J., Fu, L.-L., & Callahan, P. S. (2001). *Satellite altimetry International geophysics*, (Vol. 69, pp. 1–ii). Elsevier. [https://doi.org/10.1016/s0074-6142\(01\)80146-7](https://doi.org/10.1016/s0074-6142(01)80146-7)
- Copernicus Marine in situ TAC. (2024). Copernicus Marine in Situ - global Ocean-Delayed Mode in situ Observations of surface (drifters, HFR) and sub-surface (vessel-mounted ADCPs) water velocity. [Dataset]. SEANOE. <https://doi.org/10.17882/86236> (Accessed on 07-04-2024)
- Cornillon, P. C., Firing, E., Thompson, A., Ivanov, L., Kamenkovich, I., Buckingham, C. E., & Afanasyev, Y. (2019). Oceans. In B. Galperin & P. Read (Eds.), *Zonal jets phenomenology, genesis, and physics* (pp. 46–71). Cambridge University Press. <https://doi.org/10.1017/978107358225.003>
- Dufau, C., Orsztynowicz, M., Dibarboure, G., Morrow, R., & Le Traon, P.-Y. (2016). Mesoscale resolution capability of altimetry: Present and future. *Journal of Geophysical Research: Oceans*, 121(7), 4910–4927. <https://doi.org/10.1002/2015jc010904>
- E.U. Copernicus Marine Service Information (CMEMS). (2024a). Global ocean along track 1 3 sea surface heights NRT [Dataset]. *Marine Data Store (MDS)*. <https://doi.org/10.48670/moi-00147> (Accessed on 07-04-2024)
- E.U. Copernicus Marine Service Information (CMEMS). (2024b). Global ocean along track 1 3 sea surface heights reprocessed 1993 ongoing tailored for data assimilation [Dataset]. *Marine Data Store (MDS)*. <https://doi.org/10.48670/moi-00146> (Accessed on 07-04-2024)
- E.U. Copernicus Marine Service Information (CMEMS). (2024c). Global ocean physics reanalysis [Dataset]. *Marine Data Store (MDS)*. <https://doi.org/10.48670/moi-00021> (Accessed on 07-04-2024)
- Fablet, R., Amar, M. M., Febvre, Q., Beauchamp, M., & Chapron, B. (2021). End-to-end physics-informed representation learning for satellite ocean remote sensing data: Applications to satellite altimetry and sea surface currents. *ISPRS Annals of Photogrammetry, Remote Sensing & Spatial Information Sciences*, V-3–2021(3), 295–302. <https://doi.org/10.5194/isprs-annals-v-3-2021-295-2021>
- Fablet, R., Febvre, Q., & Chapron, B. (2023). Multimodal 4DVarNets for the reconstruction of sea surface dynamics from SST-SSH synergies. *IEEE Transactions on Geoscience and Remote Sensing*, 61, 1–14. <https://doi.org/10.1109/tgrs.2023.3268006>
- Febvre, Q. (2023). Code and data release simulation-based 4dvarnets for satellite altimetry. [Dataset]. Zenodo. <https://doi.org/10.5281/zenodo.8064113>
- Febvre, Q., Fablet, R., Le Sommer, J., & Ubelmann, C. (2022). Joint calibration and mapping of satellite altimetry data using trainable variational models. In *ICASSP 2022–2022 IEEE international conference on acoustics, speech and signal processing (ICASSP)* (pp. 1536–1540).
- Febvre, Q., Le Sommer, J., Ubelmann, C., & Fablet, R. (2024). Training neural mapping schemes for satellite altimetry with simulation data. *Journal of Advances in Modeling Earth Systems*, 16(7), e2023MS003959. <https://doi.org/10.1029/2023MS003959>
- Ferrari, R., & Wunsch, C. (2009). Ocean circulation kinetic energy: Reservoirs, sources, and sinks. *Annual Review of Fluid Mechanics*, 41(1), 253–282. <https://doi.org/10.1146/annurev.fluid.40.111406.102139>
- Fu, L.-L., Pavelsky, T., Creautx, J.-F., Morrow, R., Farrar, J. T., Vaze, P., et al. (2024). The surface water and Ocean Topography mission: A breakthrough in radar remote sensing of the ocean and land surface water. *Geophysical Research Letters*, 51(4), e2023GL107652. <https://doi.org/10.1029/2023gl107652>
- Gao, Z., Chapron, B., Ma, C., Fablet, R., Febvre, Q., Zhao, W., & Chen, G. (2024). A deep learning approach to extract balanced motions from sea surface height snapshot. *Geophysical Research Letters*, 51(7), e2023GL106623. <https://doi.org/10.1029/2023gl106623>
- Gaultier, L., Ubelmann, C., & Fu, L.-L. (2016). The challenge of using future SWOT data for oceanic field reconstruction. *Journal of Atmospheric and Oceanic Technology*, 33(1), 119–126. <https://doi.org/10.1175/jtech-d-15-0160.1>
- Goh, E., Yepremyan, A. R., Wang, J., & Wilson, B. (2023). MAESSTRO: Masked autoencoders for sea surface temperature reconstruction under occlusion. *EGUphere*, 2023, 1–20. [pre-print].
- Hoskins, B. J. (1982). The mathematical theory of frontogenesis. *Annual Review of Fluid Mechanics*, 14(1), 131–151. <https://doi.org/10.1146/annurev.fl.14.010182.001023>
- Isern-Fontanet, J., Chapron, B., Lapeyre, G., & Klein, P. (2006). Potential use of microwave sea surface temperatures for the estimation of ocean currents. *Geophysical Research Letters*, 33(24). <https://doi.org/10.1029/2006gl027801>
- Isern-Fontanet, J., Shinde, M., & González-Haro, C. (2014). On the transfer function between surface fields and the geostrophic stream function in the Mediterranean Sea. *Journal of Physical Oceanography*, 44(5), 1406–1423. <https://doi.org/10.1175/jpo-d-13-0186.1>
- Jayne, S. R., & Marotzke, J. (2002). The oceanic eddy heat transport. *Journal of Physical Oceanography*, 32(12), 3328–3345. [https://doi.org/10.1175/1520-0485\(2002\)032<3328:toeh>2.0.co;2](https://doi.org/10.1175/1520-0485(2002)032<3328:toeh>2.0.co;2)
- JPL MUR MEaSUREs Project. (2015). GHRSST level 4 MUR global foundation sea surface temperature analysis. ver. 4.1 [Dataset]. PO.DAAC. <https://doi.org/10.5067/GHGRM-4FJ04> (Accessed on 07-04-2024)
- Klein, P., Lapeyre, G., Siegelman, L., Qiu, B., Fu, L.-L., Torres, H., et al. (2019). Ocean-scale interactions from space. *Earth and Space Science*, 6(5), 795–817. <https://doi.org/10.1029/2018ea000492>
- Kugusheva, A., Bull, H., Moschos, E., Ioannou, A., Le Vu, B., & Stegner, A. (2024). Ocean satellite data fusion for high-resolution surface current maps. *Remote Sensing*, 16(7), 1182. <https://doi.org/10.3390/rs16071182>
- Lagerloef, G. S., Mitchum, G. T., Lukas, R. B., & Niiler, P. P. (1999). Tropical Pacific near-surface currents estimated from altimeter, wind, and drifter data. *Journal of Geophysical Research*, 104(C10), 23313–23326. <https://doi.org/10.1029/1999jc900197>
- Lawrence, A., & Callies, J. (2022). Seasonality and spatial dependence of mesoscale and submesoscale ocean currents from along-track satellite altimetry. *Journal of Physical Oceanography*, 52(9), 2069–2089. <https://doi.org/10.1175/jpo-d-22-0007.1>
- Le Guillou, F., Gaultier, L., Ballarotta, M., Metref, S., Ubelmann, C., Cosme, E., & Rio, M.-H. (2023). Regional mapping of energetic short mesoscale ocean dynamics from altimetry: Performances from real observations. *Ocean Science*, 19(5), 1517–1527. <https://doi.org/10.5194/os-19-1517-2023>
- Le Guillou, F., Metref, S., Cosme, E., Ubelmann, C., Ballarotta, M., Le Sommer, J., & Verron, J. (2021). Mapping altimetry in the forthcoming SWOT era by back-and-forth nudging a one-layer quasigeostrophic model. *Journal of Atmospheric and Oceanic Technology*, 38(4), 697–710. <https://doi.org/10.1175/jtech-d-20-0104.1>
- Lellouche, J.-M., Greiner, E., Bourdallé-Badie, R., Garric, G., Melet, A., Drévillon, M., et al. (2021). The copernicus global 1/12 oceanic and sea ice GLORYS12 reanalysis. *Frontiers in Earth Science*, 9, 698876.
- Le Traon, P., Nadal, F., & Duce, N. (1998). An improved mapping method of multisatellite altimeter data. *Journal of Atmospheric and Oceanic Technology*, 15(2), 522–534. [https://doi.org/10.1175/1520-0426\(1998\)015<0522:aimmom>2.0.co;2](https://doi.org/10.1175/1520-0426(1998)015<0522:aimmom>2.0.co;2)
- Manucharyan, G. E., Siegelman, L., & Klein, P. (2021). A deep learning approach to spatiotemporal sea surface height interpolation and estimation of deep currents in geostrophic ocean turbulence. *Journal of Advances in Modeling Earth Systems*, 13(1), e2019MS001965. <https://doi.org/10.1029/2019ms001965>
- Martin, S. A. (2024a). Global DL SSH [Software]. Zenodo. <https://doi.org/10.5281/zenodo.11099094> (Accessed on 01-05-2024)

- Martin, S. A. (2024b). SimVP global SSH maps 2019. [Dataset]. *Harvard DataVerse*. <https://doi.org/10.7910/DVN/H4HQGD> Accessed on 07/04/2024
- Martin, S. A., Manucharyan, G. E., & Klein, P. (2023). Synthesizing sea surface temperature and satellite altimetry observations using deep learning improves the accuracy and resolution of gridded sea surface height anomalies. *Journal of Advances in Modeling Earth Systems*, 15(5), e2022MS003589. <https://doi.org/10.1029/2022ms003589>
- Metref, S., & Ballarotta, M. (2023). Ocean data challenges: 2023a SSH mapping OSE. [https://github.com/ocean-data-challenges/2023a\\_SSH\\_mapping\\_OSE](https://github.com/ocean-data-challenges/2023a_SSH_mapping_OSE)
- Metref, S., Ballarotta, M., Le Sommer, J., Cosme, E., Albert, A., Beauchamp, M., et al. (2023). Ocean data challenges. <https://ocean-data-challenges.github.io/>
- Morrow, R., Fu, L.-L., Ardhuin, F., Benkiran, M., Chapron, B., Cosme, E., et al. (2019). Global observations of fine-scale ocean surface topography with the surface water and ocean topography (SWOT) mission. *Frontiers in Marine Science*, 6, 232. <https://doi.org/10.3389/fmars.2019.00232>
- Naveira Garabato, A. C., Yu, X., Callies, J., Barkan, R., Polzin, K. L., Frajka-Williams, E. E., et al. (2022). Kinetic energy transfers between mesoscale and submesoscale motions in the open ocean's upper layers. *Journal of Physical Oceanography*, 52(1), 75–97. <https://doi.org/10.1175/jpo-d-21-0099.1>
- OSTST. (2024). Daily NeurOST L4 sea surface height and surface geostrophic currents [Dataset]. *NASA Physical Oceanography Distributed Active Archive Center*. <https://doi.org/10.5067/NEURO-STV24> (Accessed on 07-08-2024)
- Penven, P., Halo, I., Pous, S., & Marié, L. (2014). Cyclogeostrophic balance in the Mozambique channel. *Journal of Geophysical Research: Oceans*, 119(2), 1054–1067. <https://doi.org/10.1002/2013jc009528>
- Qiu, B., Chen, S., Klein, P., Sasaki, H., & Sasai, Y. (2014). Seasonal mesoscale and submesoscale eddy variability along the north pacific subtropical countercurrent. *Journal of Physical Oceanography*, 44(12), 3079–3098. <https://doi.org/10.1175/jpo-d-14-0071.1>
- Rio, M.-H., Mulet, S., & Picot, N. (2014). Beyond GOCE for the ocean circulation estimate: Synergetic use of altimetry, gravimetry, and in situ data provides new insight into geostrophic and ekman currents. *Geophysical Research Letters*, 41(24), 8918–8925. <https://doi.org/10.1002/2014gl061773>
- Rio, M.-H., Santoleri, R., Bourdalle-Badie, R., Griffa, A., Piterbarg, L., & Taburet, G. (2016). Improving the altimeter-derived surface currents using high-resolution sea surface temperature data: A feasibility study based on model outputs. *Journal of Atmospheric and Oceanic Technology*, 33(12), 2769–2784. <https://doi.org/10.1175/jtech-d-16-0017.1>
- Sasaki, H., Klein, P., Qiu, B., & Sasai, Y. (2014). Impact of oceanic-scale interactions on the seasonal modulation of ocean dynamics by the atmosphere. *Nature Communications*, 5(1), 5636. <https://doi.org/10.1038/ncomms6636>
- Schubert, R., Gula, J., Greatbatch, R. J., Baschek, B., & Biastoch, A. (2020). The submesoscale kinetic energy cascade: Mesoscale absorption of submesoscale mixed layer eddies and frontal downscale fluxes. *Journal of Physical Oceanography*, 50(9), 2573–2589. <https://doi.org/10.1175/jpo-d-19-0311.1>
- Schubert, R., Vergara, O., & Gula, J. (2023). The open ocean kinetic energy cascade is strongest in late winter and spring. *Communications Earth & Environment*, 4(1), 450. <https://doi.org/10.1038/s43247-023-01111-x>
- Scott, R. B., & Wang, F. (2005). Direct evidence of an oceanic inverse kinetic energy cascade from satellite altimetry. *Journal of Physical Oceanography*, 35(9), 1650–1666. <https://doi.org/10.1175/jpo2771.1>
- Siegelman, L., Klein, P., Rivière, P., Thompson, A. F., Torres, H. S., Flexas, M., & Menemenlis, D. (2020). Enhanced upward heat transport at deep submesoscale ocean fronts. *Nature Geoscience*, 13(1), 50–55. <https://doi.org/10.1038/s41561-019-0489-1>
- Sinha, A., & Abernathey, R. (2021). Estimating ocean surface currents with machine learning. *Frontiers in Marine Science*, 8, 672477. <https://doi.org/10.3389/fmars.2021.672477>
- Steinberg, J. M., Cole, S. T., Drushka, K., & Abernathey, R. P. (2022). Seasonality of the mesoscale inverse cascade as inferred from global scale-dependent eddy energy observations. *Journal of Physical Oceanography*, 52(8), 1677–1691. <https://doi.org/10.1175/jpo-d-21-0269.1>
- Storer, B. A., & Aluie, H. (2023). FlowSieve: A coarse-graining utility for geophysical flows on the sphere. *Journal of Open Source Software*, 8(84), 4277. <https://doi.org/10.21105/joss.04277>
- Storer, B. A., Buzzicotti, M., Khatri, H., Griffies, S. M., & Aluie, H. (2022). Global energy spectrum of the general oceanic circulation. *Nature Communications*, 13(1), 5314. <https://doi.org/10.1038/s41467-022-33031-3>
- Storer, B. A., Buzzicotti, M., Khatri, H., Griffies, S. M., & Aluie, H. (2023). Global cascade of kinetic energy in the ocean and the atmospheric imprint. *Science Advances*, 9(51), eadi7420. <https://doi.org/10.1126/sciadv.adl7420>
- Taburet, G., Sanchez-Roman, A., Ballarotta, M., Pujo, M.-I., Legeais, J.-F., Fournier, F., et al. (2019). Duacs DT2018: 25 years of reprocessed sea level altimetry products. *Ocean Science*, 15(5), 1207–1224. <https://doi.org/10.5194/os-15-1207-2019>
- Taylor, J. R., & Thompson, A. F. (2023). Submesoscales dynamics in the upper ocean. *Annual Review of Fluid Mechanics*, 55(1), 103–127. <https://doi.org/10.1146/annurev-fluid-031422-095147>
- Thiria, S., Sorror, C., Archambault, T., Charantonis, A., Bereziat, D., Mejia, C., et al. (2023). Downscaling of ocean fields by fusion of heterogeneous observations using deep learning algorithms. *Ocean Modelling*, 182, 102174. <https://doi.org/10.1016/j.ocemod.2023.102174>
- Torres, H. S., Klein, P., Menemenlis, D., Qiu, B., Su, Z., Wang, J., et al. (2018). Partitioning ocean motions into balanced motions and internal gravity waves: A modeling study in anticipation of future space missions. *Journal of Geophysical Research: Oceans*, 123(11), 8084–8105. <https://doi.org/10.1029/2018JC014438>
- Ubelmann, C., Carrere, L., Durand, C., Dibarboure, G., Faugère, Y., Ballarotta, M., et al. (2022). Simultaneous estimation of ocean mesoscale and coherent internal tide sea surface height signatures from the global altimetry record. *Ocean Science*, 18(2), 469–481. <https://doi.org/10.5194/os-18-469-2022>
- Ubelmann, C., Dibarboure, G., Gaultier, L., Ponte, A., Ardhuin, F., Ballarotta, M., & Faugère, Y. (2021). Reconstructing ocean surface current combining altimetry and future spaceborne Doppler data. *Journal of Geophysical Research: Oceans*, 126(3), e2020JC016560. <https://doi.org/10.1029/2020JC016560>
- Ubelmann, C., Klein, P., & Fu, L.-L. (2015). Dynamic interpolation of sea surface height and potential applications for future high-resolution altimetry mapping. *Journal of Atmospheric and Oceanic Technology*, 32(1), 177–184. <https://doi.org/10.1175/jtech-d-14-00152.1>
- Uchida, T., Abernathey, R., & Smith, S. (2017). Seasonality of eddy kinetic energy in an eddy permitting global climate model. *Ocean Modelling*, 118, 41–58. <https://doi.org/10.1016/j.ocemod.2017.08.006>
- Wang, H., Grisouard, N., Salehipour, H., Nuz, A., Poon, M., & Ponte, A. L. (2022). A deep learning approach to extract internal tides scattered by geostrophic turbulence. *Geophysical Research Letters*, 49(11), e2022GL099400. <https://doi.org/10.1029/2022GL099400>
- Wunsch, C. (1999). Where do ocean eddy heat fluxes matter? *Journal of Geophysical Research*, 104(C6), 13235–13249. <https://doi.org/10.1029/1999jc000062>

- Xiao, Q., Balwada, D., Jones, C. S., Herrero-González, M., Smith, K. S., & Abernathey, R. (2023). Reconstruction of surface kinematics from sea surface height using neural networks. *Journal of Advances in Modeling Earth Systems*, 15(10), e2023MS003709. <https://doi.org/10.1029/2023ms003709>
- Yoo, J. G., Kim, S. Y., & Kim, H. S. (2018). Spectral descriptions of submesoscale surface circulation in a coastal region. *Journal of Geophysical Research: Oceans*, 123(6), 4224–4249. <https://doi.org/10.1029/2016jc012517>
- Zhang, Z., Wang, W., & Qiu, B. (2014). Oceanic mass transport by mesoscale eddies. *Science*, 345(6194), 322–324. <https://doi.org/10.1126/science.1252418>

## References From the Supporting Information

- Bretherton, F. P., Davis, R. E., & Fandry, C. (1976). A technique for objective analysis and design of oceanographic experiments applied to MODE-73. *Deep-Sea Research and Oceanographic Abstracts*, 23(7), 559–582. [https://doi.org/10.1016/0011-7471\(76\)90001-2](https://doi.org/10.1016/0011-7471(76)90001-2)
- Chin, T. M., Vazquez-Cuervo, J., & Armstrong, E. M. (2017). A multi-scale high-resolution analysis of global sea surface temperature. *Remote Sensing of Environment*, 200, 154–169. <https://doi.org/10.1016/j.rse.2017.07.029>
- Gao, Z., Tan, C., Wu, L., & Li, S. Z. (2022). SimVP: Simpler yet better video prediction. In *Proceedings of the IEEE/CVF conference on computer vision and pattern recognition (CVPR)* (pp. 3170–3180).
- Okubo, A. (1970). Horizontal dispersion of floatable particles in the vicinity of velocity singularities such as convergences. *Deep-Sea Research and Oceanographic Abstracts*, 17(3), 445–454. [https://doi.org/10.1016/0011-7471\(70\)90059-8](https://doi.org/10.1016/0011-7471(70)90059-8)
- Shi, X., Chen, Z., Wang, H., Yeung, D.-Y., Wong, W.-K., & Woo, W.-c. (2015). Convolutional LSTM network: A machine learning approach for precipitation nowcasting. *Advances in Neural Information Processing Systems*, 28.
- Tan, C., Gao, Z., Li, S., & Li, S. Z. (2022). SimVP: Towards simple yet powerful spatiotemporal predictive learning. *arXiv preprint arXiv:2211.12509*.
- Vallis, G. K. (2017). *Atmospheric and oceanic fluid dynamics*. Cambridge University Press.
- Weiss, J. (1991). The dynamics of enstrophy transfer in two-dimensional hydrodynamics. *Physica D: Nonlinear Phenomena*, 48(2–3), 273–294. [https://doi.org/10.1016/0167-2789\(91\)90088-q](https://doi.org/10.1016/0167-2789(91)90088-q)